

Continuation Based Method to Find Periodic Windows in Bifurcation Diagrams with Applications to the Chua's Circuit with a Cubic Nonlinearity

Zbigniew Galias, *Senior Member, IEEE*

Abstract—The existence of periodic windows in the parameter space is a common feature of nonlinear systems capable to produce chaotic behavior. Detection of positions of periodic windows is important both from the theoretical and practical points of view. In this work, a systematic method to detect periodic windows in bifurcation diagrams is proposed. The search method is a combination of the trajectory monitoring approach to find unstable periodic orbits and the continuation method to calculate positions of periodic windows. The method is applied to the Chua's circuit with a smooth nonlinearity. It is shown that the proposed method outperforms standard methods to find periodic windows in bifurcation diagrams.

Index Terms—bifurcation diagram, periodic window, chaos, Chua's circuit.

I. INTRODUCTION

Construction of bifurcation diagrams is one of the main tools to study the dynamics of nonlinear systems under parameter variation and to detect various bifurcation types [1], [2], [3], [4], [5], [6].

Single parameter bifurcation diagrams are constructed by plotting steady state trajectories versus the value of a selected system's parameter called the bifurcation parameter. Two-parameter and three-parameter bifurcation diagrams are obtained by finding steady state solutions in a two- or three-dimensional parameter space and plotting regions in the parameter space with different types of steady state behavior (equilibrium, period- n orbit, chaos, divergence) using different colors [7], [8].

One of the frequently observed routes leading to chaotic behavior is the period-doubling cascade [9], [10], [2], [11], [12]. In this scenario, the chaotic region starts at the accumulation point of an infinite sequence of period-doubling bifurcations. Commonly, within the chaotic region one may encounter periodic windows—regions with stable periodic behavior. Finding the positions of periodic windows is important both from the theoretical and practical points of view. Knowing the widths of periodic windows one may compute the measures of the set of regular parameters (with periodic behavior) and stochastic parameters (with chaotic behavior). Knowing the positions of periodic windows helps in selecting parameters of the system for the proper operation of chaos-based applications, including random number generators [13], chaos-based encryption [14] and secure communication [15],

[16]. Finding periodic windows, especially the narrow ones, is a challenging numerical problem [17].

The main purpose of this study is the development of efficient methods to find periodic windows in bifurcation diagrams. The proposed method is a combination of the trajectory monitoring approach to find unstable periodic orbits for a selected point in the parameter space and the continuation method to locate periodic windows in the region of interest.

As a representative example of a nonlinear system, we consider the Chua's circuit [18], which is a classical example of an electronic circuit with various types of dynamical behaviors including chaos. The Chua's circuit with a piecewise linear nonlinearity has been substantially studied over the last four decades [19], [20], [21], [22]. Bifurcation diagrams are constructed in [2]. The existence of Shilnikov and topological chaos is proved in [23] and [24]. Bifurcations diagrams are constructed for the dual Chua's system in [25].

The Chua's circuit with a third order polynomial (cubic) nonlinearity is introduced in [26]. In [27], the existence of chaos in this circuit for various parameter values is proved. The case of the double-scroll attractor is studied in [28]. In [29], a different smooth nonlinearity in the Chua's circuit is considered.

In this work, we consider the Chua's circuit with a cubic nonlinearity and study the existence of periodic windows for this system. Preliminary version of the results presented in this work are described in [30], where the study of periodic windows in a neighborhood of the point in the parameter space where the spiral attractor exists is carried out. Here, a more detailed description of the search method is presented, the Chua's circuit with a different bifurcation parameter is considered, and a more challenging case of the double-scroll attractor is investigated. In neighborhoods of points in the parameter space for which the spiral attractor and the double-scroll attractor are observed, several periodic windows are found and their properties are studied. Based on the results obtained, the dynamics of the Chua's circuit in these two regions of the parameter space is compared.

The layout of the remaining part of this paper is as follows. The definition of the Chua's circuit is given in Section II. A novel systematic method to find periodic windows is presented in Section III. Section IV presents results on the existence of periodic windows in bifurcation diagram of the smooth Chua's circuit. The results obtained are compared with the result produced by the standard method based on finding steady state behavior for selected points in the parameter

Work supported by the AGH University of Science and Technology.

Z. Galias is with the Department of Electrical Engineering, AGH University of Science and Technology, Kraków, Poland, (e-mail: galias@agh.edu.pl).

space. It is shown that the standard method fails to find narrow windows and the reasons for its failure are explained.

II. THE CHUA'S CIRCUIT

The dynamics of Chua's circuit is given by the following set of equations

$$\begin{aligned} \frac{dx}{dt} &= \frac{y-x}{RC_1} - \frac{g(x)}{C_1}, \\ \frac{dy}{dt} &= \frac{x-y}{RC_2} + \frac{z}{C_2}, \\ \frac{dz}{dt} &= -\frac{y}{L} - \frac{R_0 z}{L}. \end{aligned} \quad (1)$$

We consider the case with nonlinear function g being a cubic polynomial [26] defined by $g(x) = g_1 x + g_2 x^3$. The Chua's circuit is presented in Fig. 1.

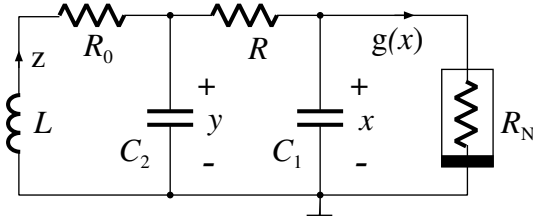


Fig. 1. The Chua's circuit.

In this study, the parameter $R \in [1.96, 2.16]$ is selected as a bifurcation parameter. Other parameters are fixed at $C_1 = 0.7$, $C_2 = 7.8$, $L = 1.891$, $R_0 = 0.01499$, $g_1 = -0.59$, and $g_2 = 0.02$. The origin $(0, 0, 0)$ is a unstable equilibrium of (1). Additionally, there exists a symmetric pair of unstable equilibria given by $\pm u^* = \pm(x^*, y^*, z^*)$, where $x^* = \sqrt{-(g_1 + (R+R_0)^{-1})g_2^{-1}}$, $y^* = R_0(R+R_0)^{-1}x^*$, and $z^* = -(R+R_0)^{-1}x^*$.

Example trajectories obtained for $R = 2.1$ and $R = 2.0$ are shown in Fig. 2. In the first case the spiral attractor is observed, while in the second case the well-known double-scroll attractor exists.

In the following, the system (1) is analyzed using the concept of a return map (also called a Poincaré map), which converts the continuous time system to a discrete time system. Let us define the set $\Sigma = \{u = (x, y, z) : |x| = x^*\}$ which is the union of two parallel planes $\Sigma_1 = \{u = (x, y, z) : x = +x^*\}$ and $\Sigma_2 = \{u = (x, y, z) : x = -x^*\}$. The set Σ is called the return set or the Poincaré section. Note that the equilibria $\pm u^*$ belong to Σ and that Σ changes with the bifurcation parameter R . The return set Σ is selected in such a way that trajectories of the continuous dynamical system (1) intersect Σ transversally. The *return map* $P : \Sigma \mapsto \Sigma$ is defined as follows. The image $P(u)$ of $u \in \Sigma$ under the return map is the first intersection point of the trajectory $\{u(t) : t > 0\}$ started at $u(0) = u$ with the return set Σ .

A trajectory $(u_k)_{k \geq 0}$ of the Poincaré map P starting at the point $u_0 \in \Sigma$ is given by $u_{k+1} = P(u_k)$, $k \geq 0$. Example trajectories of P for $R = 2.1$ and $R = 2$ are plotted in Fig. 3. In Fig. 3(b) intersections of the trajectory with the planes Σ_1 and Σ_2 are plotted using different colors.

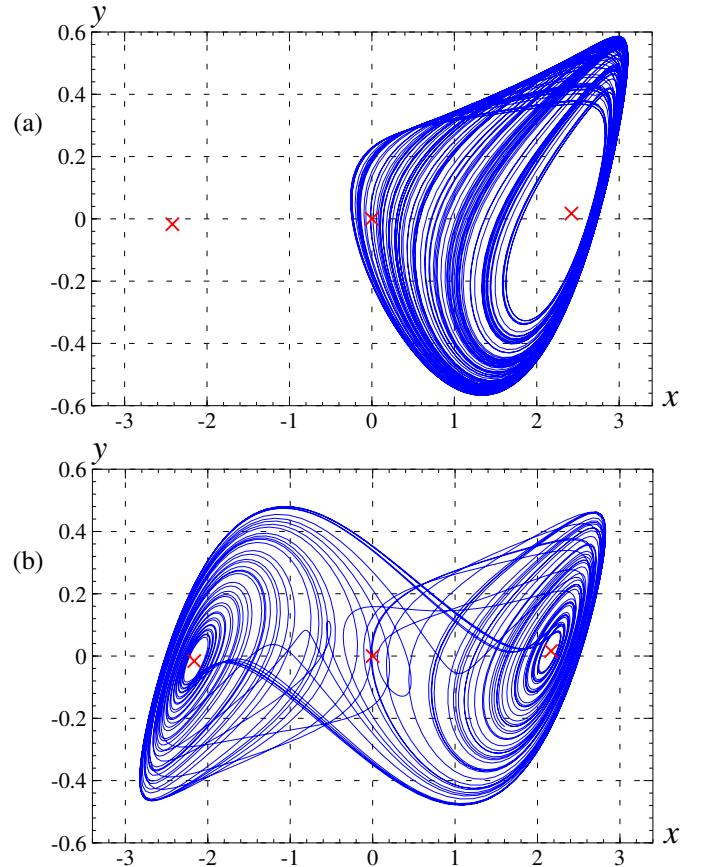


Fig. 2. Example trajectories; (a) $R = 2.1$, (b) $R = 2.0$. Equilibria are plotted using the \times symbol.

Note that iterations of the return map P correspond to intersections of trajectories of (1) with Σ in both directions. In consequence, all periodic orbits intersecting Σ transversally have periods which are even numbers. In the study of periodic orbits it is more convenient to consider intersections in a single direction only. This can be achieved by considering the Poincaré map P_+ with the return set $\Sigma_+ = \{u = (x, y, z) : |x| = x^*, x \cdot \dot{x} > 0\}$.

A bifurcation diagram for the map P_+ with the bifurcation parameter $R \in [1.96, 2.16]$ is shown in Fig. 4. 4001 values from the interval $R \in [1.96, 2.16]$ are considered. In each case, a trajectory of P_+ with the length 20000 is computed. First 10000 iterations are skipped in the hope to reach the steady state and the next 10000 iterations are plotted. For $R = 2.16$ one may see a period-2 orbit of P_+ . For smaller R the period-doubling cascade can be seen. Chaotic region starts at the end of the period-doubling cascade. In the bifurcation diagram one may see several *periodic windows*—intervals of parameter values for which the observed steady state trajectory is periodic. In Section IV, we study the existence of periodic windows in small intervals enclosing parameter values $R = 2.1$ and $R = 2.0$ for which different types of chaotic attractors are observed in simulations (compare Fig. 2).

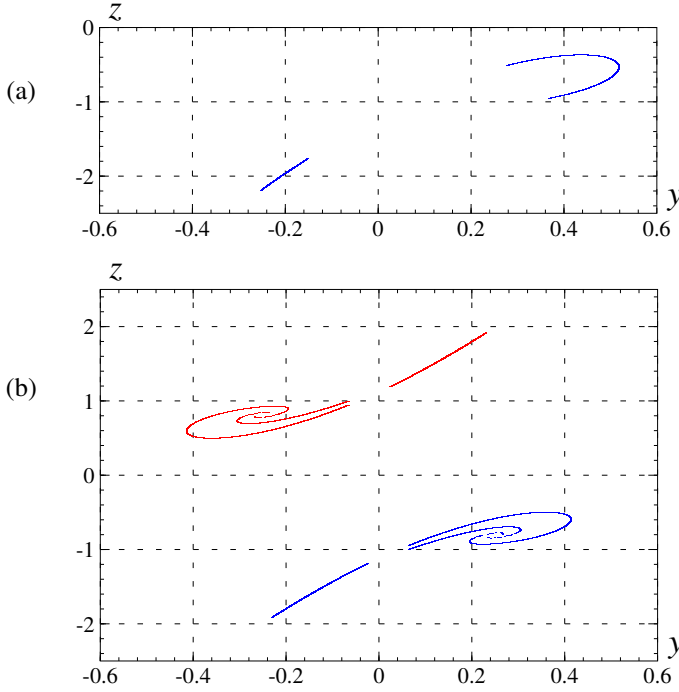


Fig. 3. Trajectories of the return map; (a) $R = 2.1$, (b) $R = 2$.

III. SEARCH FOR PERIODIC WINDOWS IN BIFURCATION DIAGRAMS

Let μ be the selected bifurcation parameter of the considered nonlinear system. We discuss the problem how to efficiently find periodic windows existing in the interval $\mu \in [\mu_{\min}, \mu_{\max}]$.

A. Brute force approach

The most frequently used method to find periodic windows is the brute force approach in which one finds steady state behavior for test parameter values belonging to the parameter range $[\mu_{\min}, \mu_{\max}]$. For each test parameter value a trajectory of a specified length is computed and its steady state is studied. If the steady state is periodic then a periodic window is found. Two parameters of this method are important for its proper operation: the length m of generated trajectories and the number n of test points. Increasing m increases the probability that a steady state is reached. Large n is required to find narrow periodic windows.

B. Continuation based approach

Let us now introduce the continuation based method to find periodic windows. In the first part of the algorithm, a parameter value $\bar{\mu}$ in the interval $[\mu_{\min}, \mu_{\max}]$ is selected and unstable periodic orbits existing for this parameter value are found using the method of *close returns*. In this method, a long trajectory $(u_k)_{k=0}^{m-1}$ is computed and δ -pseudo periodic orbits are found. δ -pseudo periodic orbit with the period p is a part of a trajectory $\psi_{n,p} = (u_k)_{k=n}^{n+p-1}$ such that the condition $\|u_{n+p} - u_n\| \leq \delta$ is satisfied. Next, accurate positions of periodic orbits are calculated using the Newton method. To

investigate periodic orbits of P we consider the map F defined by

$$F \begin{pmatrix} u_0 \\ u_1 \\ \dots \\ u_{p-1} \end{pmatrix} = \begin{pmatrix} P(u_0) - u_1 \\ P(u_1) - u_2 \\ \dots \\ P(u_{p-1}) - u_0 \end{pmatrix}. \quad (2)$$

It is clear that if $F(\xi) = 0$, where $\xi = (u_0, u_1, \dots, u_{p-1})$ then $P^p(u_0) = u_0$, which means that ξ is a period- p orbit of P . For each δ -pseudo periodic orbits $\psi_{n,p}$ the Newton operator

$$N(\xi) = \xi - (F'(\xi))^{-1} F(\xi). \quad (3)$$

is applied iteratively $\xi_{n+1} = N(\xi_n)$ with the initial condition $\xi_0 = \psi_{n,p}$. The convergence of the Newton method indicates that a periodic orbit exists in a neighborhood of the δ -pseudo periodic orbit. The Newton method to find a periodic orbit starting from the initial condition ξ is presented as the Algorithm 1. The convergence of the Newton operator is controlled by the parameter $\varepsilon_{\text{newton}}$. The maximum allowed distance from the initial orbit is controlled by the parameter d_{max} .

Algorithm 1 Newton method

Input: μ is the parameter value
Input: ξ is the initial guess of the position of the orbit
Output: on success ξ' is an accurate position of the orbit

- 1: **function** NEWTON(μ, ξ, ξ')
- 2: $\xi' \leftarrow \xi$
- 3: **for** $i = 1, 2, \dots, n_{\text{newton}}$ **do**
- 4: $h \leftarrow (F'(\xi'))^{-1} F(\xi')$ $\triangleright F$ depends on μ
- 5: $\xi' \leftarrow \xi' - h$ \triangleright Newton iteration
- 6: **if** $\|h\| \leq \varepsilon_{\text{newton}}$ **then** \triangleright convergence achieved
- 7: **return true**
- 8: **end if**
- 9: **if** $\|\xi' - \xi\| > d_{\text{max}}$ **then** $\triangleright \xi'$ is too far from ξ
- 10: **return false** \triangleright no convergence
- 11: **end if**
- 12: **end for**
- 13: **return false** \triangleright too many iterations
- 14: **end function**

The procedure to find periodic orbits for a given parameter value μ using the method of close returns is presented as the Algorithm 2. In the algorithm m is the length of the generated trajectory and p_{max} is the maximum period of the orbits to be detected. Accurate positions of periodic orbits are used to check what is the minimal period of each orbit and to generate the list S of unique periodic orbits existing for the selected parameter value μ .

In the second part of the algorithm the continuation method is applied for each unstable periodic orbit to find periodic windows in $\mu \in [\mu_{\min}, \mu_{\max}]$. Let $\xi_{\bar{\mu}} = (u_k)_{k=0}^{p-1}$ be a periodic orbit existing for $\bar{\mu}$. The parameter value $\mu = \bar{\mu}$ and the position of the orbit $\xi_{\mu} = \xi_{\bar{\mu}}$ are the initial values for the continuation method. During the algorithm μ is modified by $\Delta\mu$ (increased or decreased) until the endpoint of $[\mu_{\min}, \mu_{\max}]$ is reached or a periodic window is found. After each parameter change the Newton method is applied to find the position of the orbit for the tested value $\mu' = \mu + \Delta\mu$ of the

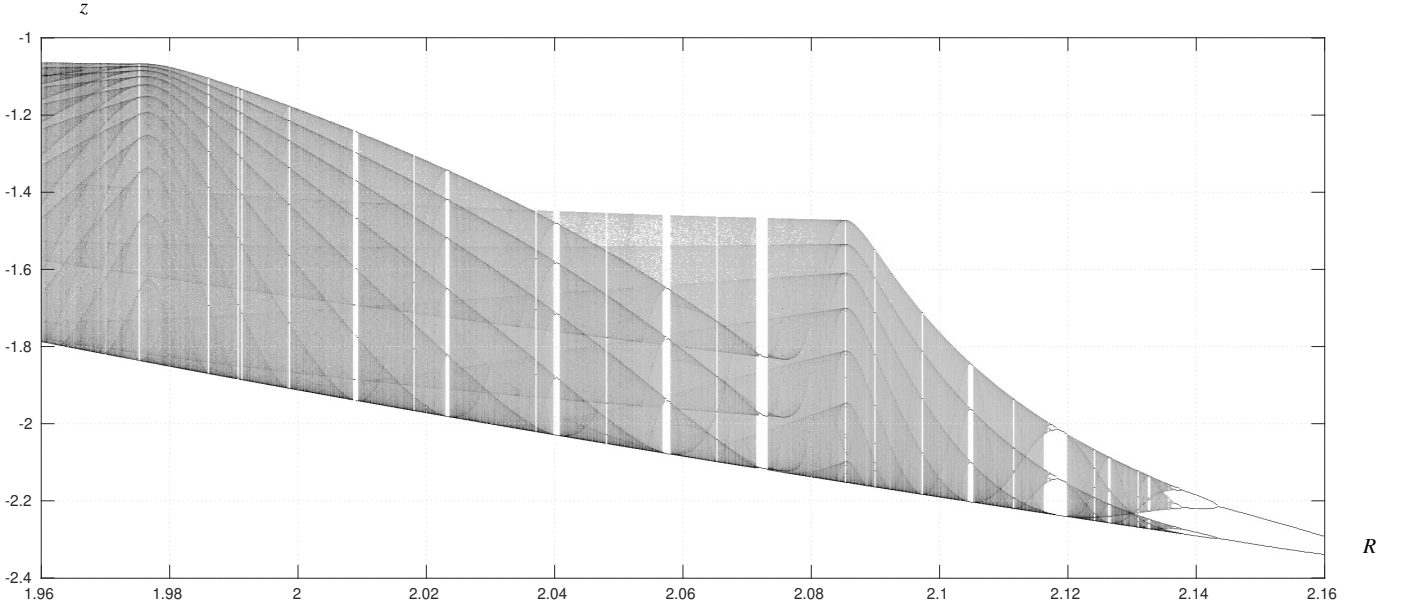


Fig. 4. Bifurcation diagram of P_+ , $R \in [1.96, 2.16]$.

Algorithm 2 Find periodic orbits.

Input: μ is the parameter value
Output: S is the set of periodic orbits found for μ

```

1: procedure FINDPERORBITS( $\mu, S$ )
2:   Select  $u_0$ 
3:    $S \leftarrow \emptyset$ 
4:   for  $i = 1, 2, \dots, m-1$  do
5:      $u_k \leftarrow P(u_{k-1})$   $\triangleright P$  depends on  $\mu$ 
6:     for  $p = 1, 2, \dots, p_{\max}$  do
7:       if  $k \geq p$  and  $\|u_k - u_{k-p}\| < \delta$  then
8:          $\xi \leftarrow (u_{k-p}, u_{k-p+1}, \dots, u_{k-1})$ 
9:         if NEWTON( $\mu, \xi, \xi'$ ) then
10:           $S \leftarrow S \cup \{\xi'\}$ 
11:        end if
12:      end if
13:    end for
14:  end for
15: end procedure

```

parameter. If the Newton method does not converge or if the Newton method converges to a periodic orbit located far from ξ_μ then the computations are repeated for a smaller step size $\Delta\mu$. In the opposite case the parameter value and the position of the orbit are updated, the step size $\Delta\mu$ is increased and the stability of ξ_μ is studied. If the orbit is stable then the computations are stopped because a periodic window is found. The computations are also stopped when μ is outside $[\mu_{\min}, \mu_{\max}]$, or $\Delta\mu$ is smaller than the minimum step size Δ_{\min} . The procedure to find a periodic window using the continuation method starting at the parameter value μ and the periodic orbit ξ existing for this parameter value is presented as the Algorithm 3. The initial value of the step size is controlled by the parameter $\Delta_0 > 0$. The search direction is defined by the sign of the parameter d .

Algorithm 3 Find a periodic window.

Input: μ is the parameter value
Input: ξ is the position of a periodic orbit for μ
Input: $d = \pm 1$ defines the search direction
Output: on success $[\mu_1, \mu_2]$ is a periodic window

```

1: function FINDPERWIN( $\mu, \xi, d, \mu_1, \mu_2$ )
2:    $\Delta\mu \leftarrow \text{sgn}(d) \cdot \Delta_0$   $\triangleright$  select direction
3:   while  $|\Delta\mu| > \Delta_{\min}$  and  $\mu \in [\mu_{\min}, \mu_{\max}]$  do
4:     if NEWTON( $\mu + \Delta\mu, \xi, \xi'$ ) and  $\|\xi - \xi'\| \leq \varepsilon$  then
5:        $\mu \leftarrow \mu + \Delta\mu$ 
6:        $\xi \leftarrow \xi'$ 
7:       if ISSTABLE( $\mu, \xi$ ) then  $\triangleright$  window found
8:         FINDPERWINENDPOINT( $\mu, \xi, -1, \mu_1$ )
9:         FINDPERWINENDPOINT( $\mu, \xi, +1, \mu_2$ )
10:      return true
11:     end if
12:      $\Delta\mu \leftarrow 1.2 * \Delta\mu$ 
13:   else
14:      $\Delta\mu \leftarrow 0.5 * \Delta\mu$ 
15:   end if
16: end while
17: return false
18: end function

```

Once a stable periodic orbit is detected the continuation method is applied in both directions to find endpoints of the corresponding periodic window. The initial values for the continuation method are the parameter value μ for which the stable periodic orbit exists and the position ξ of the stable periodic orbit. When finding endpoints of periodic windows the tested parameter value $\mu' = \mu + \Delta\mu$ is accepted if the Newton method converges and the periodic orbit is stable. Otherwise, the computations are repeated for a smaller step size $\Delta\mu$. The procedure to find one of the endpoints of

a periodic window is presented as the Algorithm 4. The input parameter d is used to select which endpoint is being computed.

Algorithm 4 Find periodic window endpoint.

Input: μ belonging to a periodic window
Input: ξ is the position of a stable periodic orbit
Output: μ_{end} is a periodic window endpoint

```

1: procedure FINDPERWINENDPOINT( $\mu, \xi, d, \mu_{\text{end}}$ )
2:    $\mu_{\text{end}} \leftarrow \mu$ 
3:    $\Delta\mu \leftarrow \text{sgn}(d) \cdot \Delta_0$   $\triangleright$  select direction
4:   while  $|\Delta\mu| > \Delta_{\text{min}}$  and  $\mu_{\text{end}} \in [\mu_{\text{min}}, \mu_{\text{max}}]$  do
5:     if NEWTON( $\mu_{\text{end}} + \Delta\mu, \xi, \xi'$ ) and  $\|\xi - \xi'\| \leq \varepsilon$ 
6:       and ISSTABLE( $\mu_{\text{end}} + \Delta\mu, \xi'$ ) then
7:          $\mu_{\text{end}} \leftarrow \mu_{\text{end}} + \Delta\mu$ 
8:          $\xi \leftarrow \xi'$ 
9:          $\Delta\mu \leftarrow 1.2 \cdot \Delta\mu$ 
10:      else
11:         $\Delta\mu \leftarrow 0.5 \cdot \Delta\mu$ 
12:      end if
13:    end while
14: end procedure

```

The complete procedure to find periodic windows in the parameter range $[\mu_{\text{min}}, \mu_{\text{max}}]$ is presented as the Algorithm 5. In this procedure one first finds unstable periodic orbits existing for μ_{min} and μ_{max} and then looks for periodic windows by continuing periodic orbits in the correct direction. It is possible to select additional points in the parameter range $[\mu_{\text{min}}, \mu_{\text{max}}]$ (for example the middle point) and start the continuation from there. In this case one should continue periodic orbits in both directions. The procedure is completed after processing all unstable periodic orbits found in the first part of the algorithm.

Algorithm 5 Find periodic windows in $[\mu_{\text{min}}, \mu_{\text{max}}]$.

Input: $[\mu_{\text{min}}, \mu_{\text{max}}]$ is the parameter range
Output: W the set of periodic windows

```

1: function FINDPERWINDOWS( $\mu_{\text{min}}, \mu_{\text{max}}, W$ )
2:    $W \leftarrow \emptyset$   $\triangleright$  the set of periodic windows
3:   FINDPERORBITS( $\mu_{\text{min}}, S$ )
4:   for  $\xi \in S$  do
5:     if FINDPERWIN( $\mu_{\text{min}}, \xi, +1, \mu_1, \mu_2$ ) then
6:        $W \leftarrow W \cup \{[\mu_1, \mu_2]\}$ 
7:     end if
8:   end for
9:   FINDPERORBITS( $\mu_{\text{max}}, S$ )
10:  for  $\xi \in S$  do
11:    if FINDPERWIN( $\mu_{\text{max}}, \xi, -1, \mu_1, \mu_2$ ) then
12:       $W \leftarrow W \cup [\mu_1, \mu_2]$ 
13:    end if
14:  end for
15: end function

```

IV. PERIODIC WINDOWS FOR THE CHUA'S CIRCUIT

Here, we present results on the existence of periodic windows for the Chua's circuit close to the parameter values

$R = 2.1$ and $R = 2$. The latter case is more challenging due to the fact that the double scroll attractor is singular in the sense that it contains the origin—an unstable equilibrium. As a consequence some trajectories belonging to the attractor stay close to the origin for a long time and in consequence the time needed to return to the transversal section Σ defining the return map may be very large. This results in numerical problems when evaluating the Newton operator and using the continuation method.

A. Brute force approach

Bifurcation diagrams of P_+ for intervals $R \in [2.09, 2.11]$ and $R \in [1.99, 2.01]$ are plotted in Fig. 5. In the following n denotes the number of test parameter values selected from a given interval, N denotes the number of test parameter values for which the steady state trajectory is periodic, and W denotes the number of periodic windows detected. In each case $n = 2001$ equidistant parameter values are selected and trajectories of the length $m = 20000$ are computed. The second half of each trajectory is used to plot bifurcation diagrams. One can see several relatively wide periodic windows.

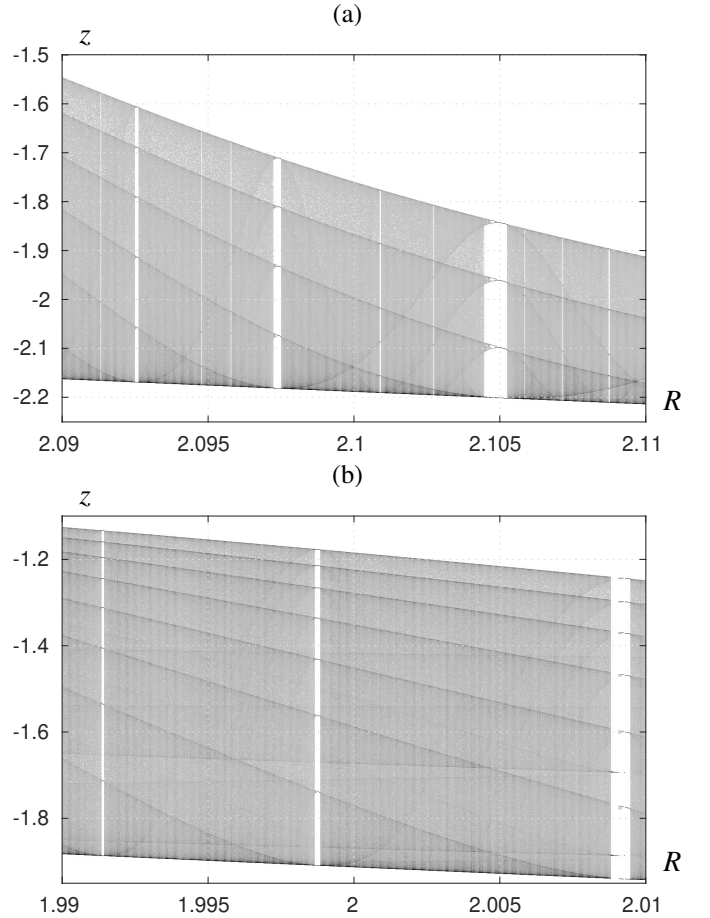


Fig. 5. Bifurcation diagrams of P_+ ; (a) $R \in [2.09, 2.11]$, (b) $R \in [1.99, 2.01]$.

More detailed bifurcation diagrams for $R \in [2.099, 2.101]$ and $R \in [1.999, 2.001]$ computed with $n = 2001$ test parameter values are shown in Fig. 6. Fewer periodic windows

than in Fig. 5 can be seen and in general periodic windows are narrower. In the first case ($R \in [2.099, 2.101]$) the steady-state trajectory is periodic in $N = 38$ cases and $W = 12$ periodic windows are detected. For the interval $R \in [1.999, 2.001]$ only for a single parameter value the observed trajectory is eventually periodic and one periodic window is found.

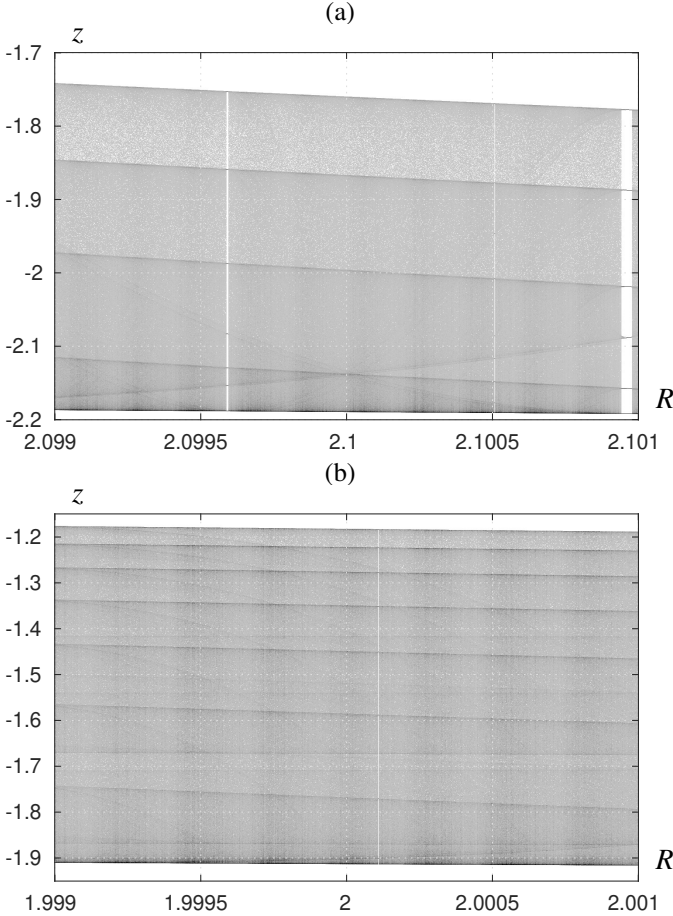


Fig. 6. Bifurcation diagrams of P_+ ; (a) $R \in [2.099, 2.101]$, (b) $R \in [1.999, 2.001]$.

To detect more periodic windows the computations are repeated with larger n . The results obtained for $n = 1001, 2001, 10001, 100001$ are given in Table I. The number of periodic windows found in the intervals $R \in [2.099, 2.101]$ and $R \in [1.999, 2.001]$ is $W = 51$ and $W = 12$, respectively.

It will be shown that the number of periodic windows is much larger. There are two reasons for which the brute force approach may fail to find more periodic windows. The first one is related to the width of periodic windows. Most low-period windows existing in the intervals $R \in [2.099, 2.101]$ and $R \in [1.999, 2.001]$ are very narrow. It follows that one has to select a large number n of test parameter values to detect such windows. As an example, let us assume that the window in the parameter range $R \in [2.099, 2.101]$ has the width $w = 10^{-10}$. In this case, one has to use $n \geq 2 \times 10^7$ to ensure that at least one test parameter value belongs to this window.

The second reason is related to a possibly long time needed for a trajectory to converge to a periodic attractor. We will

TABLE I
PERIODIC WINDOWS FOUND FOR $R \in [2.099, 2.101]$ AND $R \in [1.999, 2.001]$ USING THE BRUTE FORCE APPROACH, n IS THE NUMBER OF TEST POINTS, N IS THE NUMBER OF TEST POINTS WITH A PERIODIC STEADY STATE, W IS THE NUMBER OF PERIODIC WINDOWS FOUND, w_{total} IS THE TOTAL WIDTH OF PERIODIC WINDOWS FOUND, t IS THE COMPUTATION TIME

| n | N | W | w_{total} | t [s] |
|------------------------|------|-----|------------------------|-----------|
| $R \in [2.099, 2.101]$ | | | | |
| 1001 | 21 | 10 | 3.489×10^{-5} | 1217.79 |
| 2001 | 38 | 12 | 3.512×10^{-5} | 3107.36 |
| 10001 | 176 | 24 | 3.606×10^{-5} | 12682.50 |
| 100001 | 1702 | 51 | 4.126×10^{-5} | 128700.12 |
| $R \in [1.999, 2.001]$ | | | | |
| 1001 | 0 | 0 | 0 | 1883.01 |
| 2001 | 1 | 1 | 1.418×10^{-7} | 4424.43 |
| 10001 | 3 | 2 | 3.782×10^{-7} | 19468.14 |
| 100001 | 48 | 12 | 1.012×10^{-6} | 212952.26 |

show that in many cases the average convergence time to reach a periodic attractor existing in $R \in [2.099, 2.101]$ is well above 10^5 . The length $m = 20000$ of trajectories used in the computations presented above is not sufficient to detect these attractors.

B. Unstable periodic orbits

In the remaining part of this section, we find periodic windows existing in the parameter ranges $R \in [2.099, 2.101]$ and $R \in [1.999, 2.001]$ using the approach presented in Section III-B. In the first step of this approach for selected parameter values unstable periodic orbits are found. The search for δ -pseudo periodic orbits is carried out for the maximum period $p_{\text{max}} = 20$ and with the parameter $\delta = 0.01$. Accurate positions of unstable periodic orbits are found using the Newton method. These results are used to verify whether the period of the orbit found is minimal and to select unique periodic orbits from the set of candidates. The number of unstable periodic orbits found for endpoints and midpoints of the ranges $R \in [2.099, 2.101]$ and $R \in [1.999, 2.001]$ are reported in Table II.

For $R \in \{2.099, 2.1, 2.101\}$ the length of the trajectory used in the method of close returns is $m = 2 \times 10^7$. As an example let us discuss the case $R = 2.099$, for which 49939 unstable periodic orbits are found. Fig. 7(a) shows how the number of periodic orbits grows with m . One can see that the plots become flat when m grows. The length m of the trajectory which has to be considered to detect all periodic orbits of a given period p grows with p . During the last 6×10^6 iterations no cycles with periods $p \leq 17$ are revealed. Therefore, one can expect that for $R = 2.099$ there is no other periodic orbit with the period $p \leq 17$.

For $R \in \{1.999, 2, 2.001\}$ the length of the trajectory used in the method of close returns is $m = 10^8$. The number of periodic orbits found is almost 10 times larger than for $R \in [2.099, 2.101]$. This confirms that the dynamics of the Chua's circuit in a neighborhood of the double-scroll attractor is much more complicated than in a neighborhood of the spiral attractor. Let us consider the case $R = 2.001$ for which 382596 unstable periodic orbits are found. Fig. 7(b) shows how the number of periodic orbits found changes with m . For $p \geq 10$

TABLE II
THE NUMBER OF UNSTABLE PERIODIC ORBITS FOUND FOR DIFFERENT VALUES OF R .

| p | $R=2.099$ | $R=2.1$ | $R=2.101$ | $R=1.999$ | $R=2$ | $R=2.001$ |
|-----------|-----------|---------|-----------|-----------|--------|-----------|
| 1 | 1 | 1 | 1 | 2 | 2 | 2 |
| 2 | 1 | 1 | 1 | 2 | 2 | 2 |
| 3 | 2 | 2 | 2 | 6 | 6 | 6 |
| 4 | 3 | 3 | 3 | 10 | 10 | 10 |
| 5 | 4 | 4 | 4 | 20 | 20 | 20 |
| 6 | 7 | 7 | 5 | 47 | 47 | 51 |
| 7 | 14 | 12 | 12 | 120 | 120 | 128 |
| 8 | 20 | 20 | 18 | 274 | 274 | 286 |
| 9 | 38 | 34 | 32 | 648 | 640 | 679 |
| 10 | 66 | 60 | 54 | 1473 | 1437 | 1549 |
| 11 | 118 | 104 | 96 | 3005 | 2934 | 3267 |
| 12 | 202 | 182 | 161 | 5390 | 5256 | 5917 |
| 13 | 366 | 322 | 288 | 8874 | 8579 | 9773 |
| 14 | 645 | 568 | 498 | 13781 | 13039 | 14751 |
| 15 | 1164 | 1010 | 884 | 20719 | 19415 | 21903 |
| 16 | 2093 | 1799 | 1554 | 29632 | 27560 | 31379 |
| 17 | 3794 | 3230 | 2772 | 40696 | 39295 | 44718 |
| 18 | 6843 | 5785 | 4905 | 55065 | 53203 | 61059 |
| 19 | 12428 | 10420 | 8739 | 71516 | 69589 | 82112 |
| 20 | 22130 | 18532 | 15272 | 89826 | 88739 | 104984 |
| ≤ 20 | 49939 | 42096 | 35301 | 341106 | 330167 | 382596 |

plots do not stabilize when m increases. Thus, one can expect that more periodic orbits exist for $p \geq 10$.

C. Continuation based method for $R \in [2.099, 2.101]$

Unstable periodic orbits existing for $R = 2.099$ are continued by increasing R to find periodic windows within the range $R \in [2.099, 2.101]$. In Table III, the results obtained for periods $p \leq 20$ are shown. W is the number of periodic windows and w_{total} is the total width of periodic windows with the period p . We also report the minimum width w_{min} and the maximum width w_{max} . Similar computations are also done for $R = 2.101$. All unstable periodic orbits existing for $R = 2.101$ can be continued by decreasing R past $R = 2.099$. In consequence, these computations do not reveal any periodic windows within the range $R \in [2.099, 2.101]$.

TABLE III
PERIOD WINDOWS EXISTING FOR $R \in [2.099, 2.101]$, W IS THE NUMBER OF PERIODIC WINDOWS, w_{total} IS THE TOTAL WIDTH.

| p | W | w_{total} | w_{min} | w_{max} |
|-----------|------|------------------------|-------------------------|-------------------------|
| 6 | 1 | 1.584×10^{-5} | 1.584×10^{-5} | 1.584×10^{-5} |
| 7 | 1 | 2.711×10^{-6} | 2.711×10^{-6} | 2.711×10^{-6} |
| 8 | 1 | 4.478×10^{-7} | 4.478×10^{-7} | 4.478×10^{-7} |
| 9 | 3 | 4.138×10^{-7} | 7.332×10^{-8} | 2.129×10^{-7} |
| 10 | 6 | 4.149×10^{-7} | 1.215×10^{-8} | 2.756×10^{-7} |
| 11 | 11 | 1.382×10^{-7} | 1.997×10^{-9} | 4.217×10^{-8} |
| 12 | 21 | 7.951×10^{-6} | 3.299×10^{-10} | 7.896×10^{-6} |
| 13 | 39 | 5.298×10^{-8} | 5.435×10^{-11} | 1.351×10^{-8} |
| 14 | 74 | 1.387×10^{-6} | 8.980×10^{-12} | 1.357×10^{-6} |
| 15 | 140 | 1.557×10^{-8} | 1.490×10^{-12} | 2.029×10^{-9} |
| 16 | 269 | 2.371×10^{-7} | 2.500×10^{-13} | 2.238×10^{-7} |
| 17 | 510 | 5.395×10^{-9} | 4.974×10^{-14} | 2.901×10^{-10} |
| 18 | 960 | 5.038×10^{-7} | 9.770×10^{-15} | 2.934×10^{-7} |
| 19 | 1657 | 2.128×10^{-9} | $< 10^{-15}$ | 2.341×10^{-10} |
| 20 | 2595 | 2.094×10^{-7} | $< 10^{-15}$ | 1.376×10^{-7} |
| ≤ 20 | 6288 | 6.066×10^{-5} | $< 10^{-15}$ | 1.584×10^{-5} |

For small periods ($p \leq 11$) the number of periodic windows in the interval $R \in [2.099, 2.101]$ is equal to the half of the

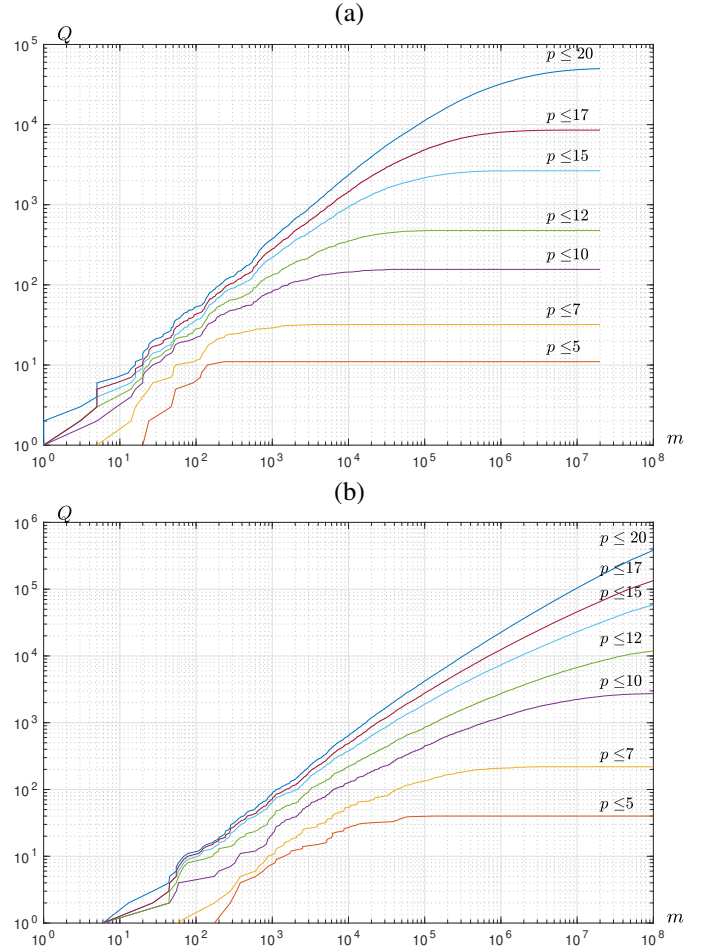


Fig. 7. The number of period- p orbits found versus the length m of the monitored trajectory; (a) $R = 2.099$, (b) $R = 2.001$.

difference between the number of periodic orbits existing for $R = 2.099$ and $R = 2.101$. This relation is also satisfied approximately for $12 \leq p \leq 17$. A similar phenomenon is observed in bifurcation diagrams of the logistic map (compare [31]), which indicates that periodic windows emerge in a similar fashion for these two systems.

In total, 6288 periodic windows found. This shows that the proposed method outperforms the brute force approach, where only 51 windows are identified. The total width $w_{\text{total}} = 6.066 \times 10^{-5}$ of periodic windows with period $p \leq 20$ is a lower bound of the measure of the set of regular parameters. From the fact that w_{total} is less than 2% of the width of the interval $R \in [2.099, 2.101]$ it follows that the Chua's circuit in this region is mostly chaotic. Let us recall that for $R = 2.1$ the spiral attractor is obtained in simulations. The closest periodic attractor found is the period-17 cycle existing for $R = 2.100000225456$. The width of the corresponding window is $w \approx 5 \times 10^{-14}$.

Example periodic attractors existing in the range $R \in [2.099, 2.101]$ are shown in Fig. 8. For each period- p window with $p \leq 10$ a parameter value in this window is selected and the corresponding periodic attractor is plotted.

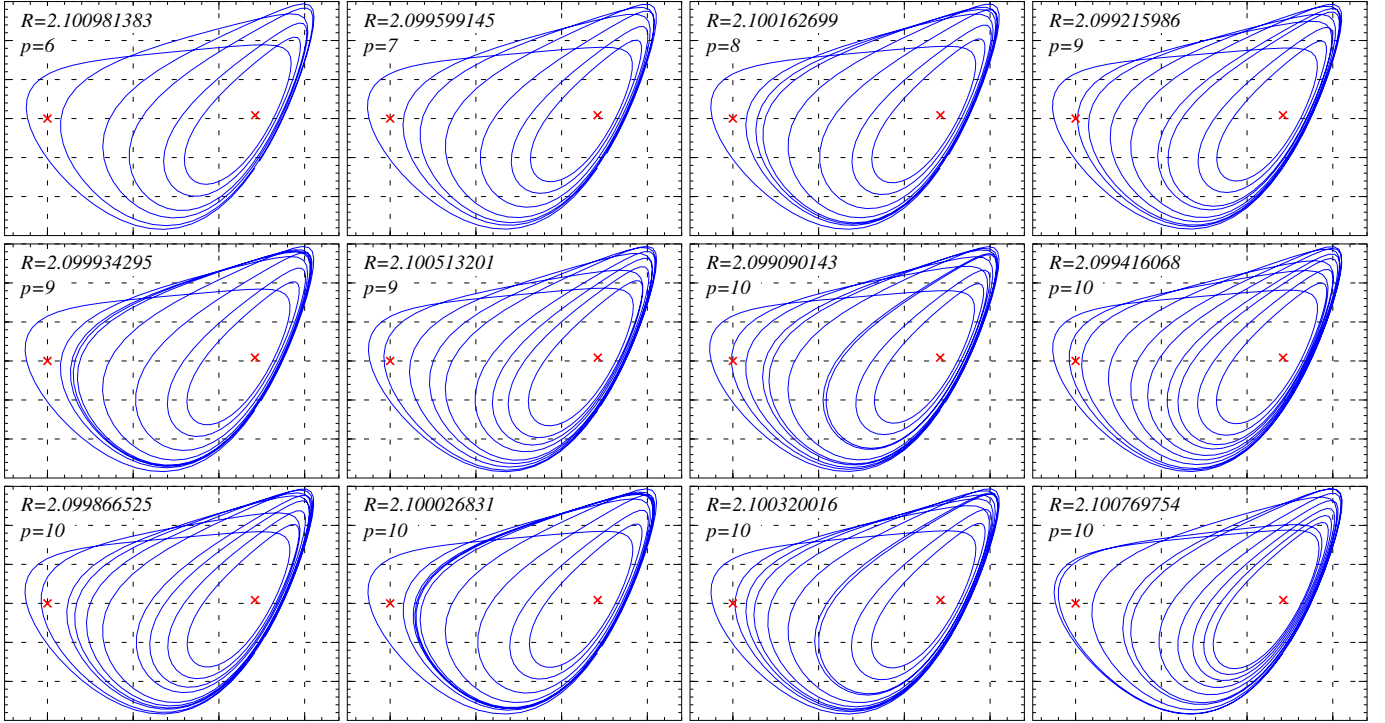


Fig. 8. Examples of low period attractors existing for $R \in [2.009, 2.101]$; variable ranges: $x \in [-0.5, 3.4]$, $y \in [-0.6, 0.6]$.

D. Continuation based method for $R \in [1.999, 2.001]$

Similar calculations are carried out to locate periodic windows for $R \in [1.999, 2.001]$. Unstable periodic orbits found for $R = 1.999$, $R = 2$, and $R = 2.001$ are continued to find positions of periodic windows within the interval $R \in [1.999, 2.001]$. In this case all three initial points in the parameter space produce some periodic windows opposite to the results obtained for the range $R \in [2.099, 2.101]$. The combined results are shown in Table IV. 3397 periodic windows with periods $p \leq 20$ are found. The results confirm that the continuation based method outperforms the brute force approach (12 periodic windows located). The minimum distance from the point $R = 2.0$ with the double-scroll attractor and the periodic window found is $d \approx 6.77 \times 10^{-7}$. A period-20 attractor exists for $R = 1.999999323223811$.

The total width of periodic windows is $w_{\text{total}} = 1.359 \times 10^{-6}$, which is approximately 45 times smaller than the total width of periodic windows found in the range $R \in [2.099, 2.101]$. The widest periodic window is observed for the period $p = 15$. Its width is $w = 2.364 \times 10^{-7}$, which is two orders of magnitude smaller than the width of the widest periodic window existing in the range $R \in [2.099, 2.101]$. In general, periodic windows in the range $R \in [1.999, 2.001]$ are narrower than in the range $R \in [2.099, 2.101]$. The results presented in Table IV confirm that the Chua's circuit for $R \in [1.999, 2.001]$ is "more chaotic" than for $R \in [2.099, 2.101]$.

Example periodic attractors existing in the range $R \in [1.999, 2.001]$ are shown in Fig. 9. The first 14 attractors are selected from periodic windows with periods $p \leq 9$. The last two attractors are selected from the widest periodic windows with periods 14 and 15, respectively. All periodic attractors

TABLE IV
PERIOD WINDOWS EXISTING FOR $R \in [1.999, 2.001]$, W IS THE NUMBER OF PERIODIC WINDOWS, w_{total} IS THE TOTAL WIDTH.

| p | W | w_{total} | w_{min} | w_{max} |
|-----------|------|-------------------------|-------------------------|-------------------------|
| 6 | 1 | 1.407×10^{-10} | 1.407×10^{-10} | 1.407×10^{-10} |
| 7 | 2 | 1.736×10^{-11} | 5.420×10^{-12} | 1.194×10^{-11} |
| 8 | 3 | 1.510×10^{-12} | 2.398×10^{-13} | 6.799×10^{-13} |
| 9 | 8 | 3.159×10^{-11} | 1.021×10^{-14} | 3.123×10^{-11} |
| 10 | 16 | 1.460×10^{-10} | $< 10^{-15}$ | 1.133×10^{-10} |
| 11 | 26 | 2.208×10^{-10} | $< 10^{-15}$ | 1.053×10^{-10} |
| 12 | 56 | 9.373×10^{-8} | $< 10^{-15}$ | 9.253×10^{-8} |
| 13 | 99 | 1.131×10^{-7} | $< 10^{-15}$ | 1.108×10^{-7} |
| 14 | 158 | 1.715×10^{-7} | $< 10^{-15}$ | 1.418×10^{-7} |
| 15 | 235 | 2.399×10^{-7} | $< 10^{-15}$ | 2.364×10^{-7} |
| 16 | 343 | 1.857×10^{-8} | $< 10^{-15}$ | 1.250×10^{-8} |
| 17 | 396 | 1.229×10^{-8} | $< 10^{-15}$ | 9.783×10^{-9} |
| 18 | 542 | 1.723×10^{-8} | $< 10^{-15}$ | 1.116×10^{-8} |
| 19 | 665 | 1.317×10^{-9} | $< 10^{-15}$ | 7.557×10^{-10} |
| 20 | 847 | 1.136×10^{-8} | $< 10^{-15}$ | 9.913×10^{-9} |
| ≤ 20 | 3397 | 1.359×10^{-6} | $< 10^{-15}$ | 2.364×10^{-7} |

visit both parts of the state space. Note that the last two periodic attractors are located further away from the origin than other attractors shown in Fig. 9. Another observation is that they visit a small neighborhood of other unstable equilibria. This may be an explanation of stability properties of these periodic attractors and widths of the corresponding periodic windows.

E. Convergence to periodic attractors

Let us assume that for a selected parameter value a periodic attractor of the return map exists. For a given initial point u , let us define the convergence time $\tau(u)$ as the number of iterations of the return map needed for the trajectory started

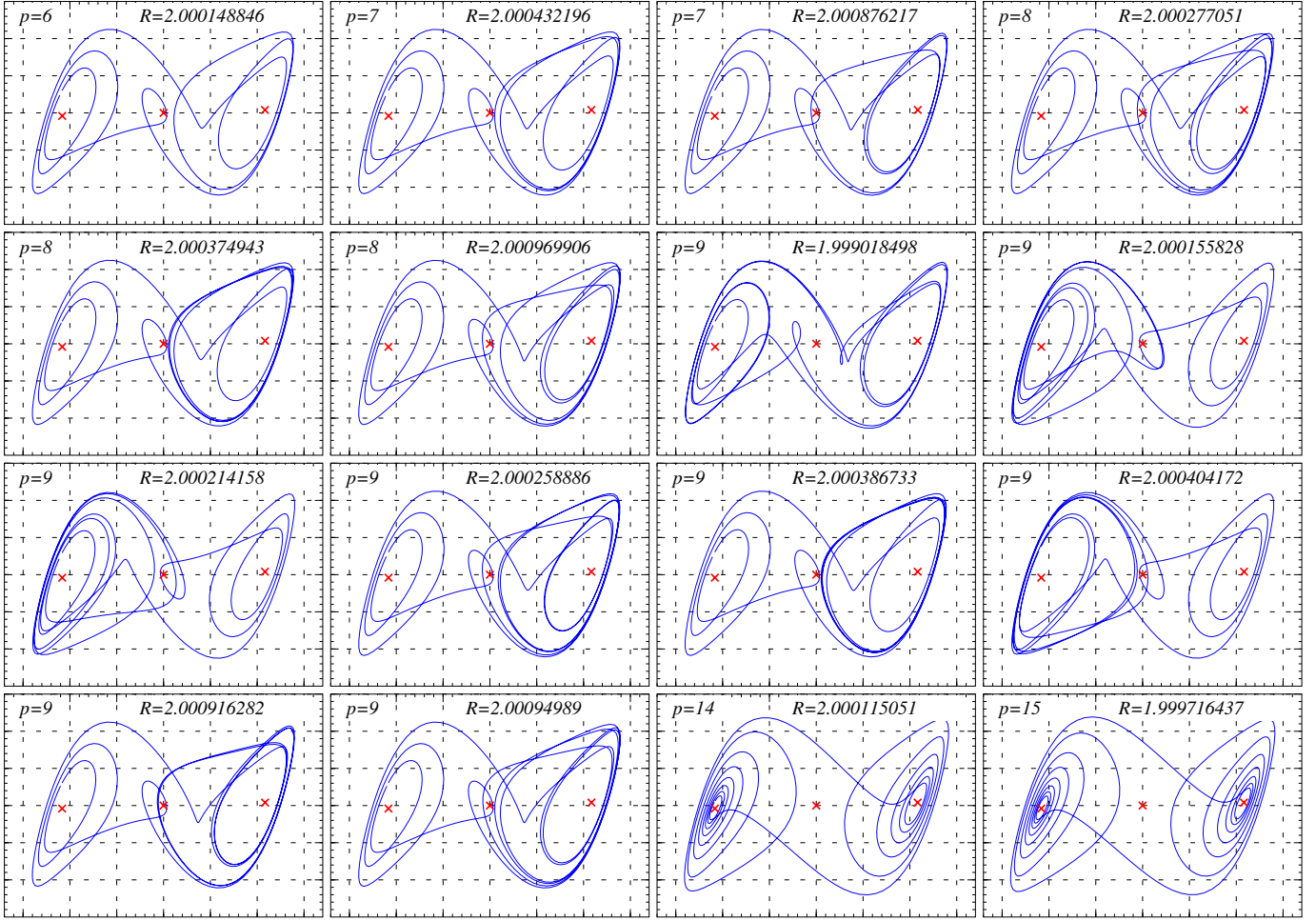


Fig. 9. Examples of low period attractors existing for $R \in [1.999, 2.001]$; variable ranges: $x \in [-3.4, 3.4]$, $y \in [-0.6, 0.6]$.

at u to converge to the periodic attractor. Clearly, the convergence time $\tau(u)$ depends on the initial point u . Immediate convergence is observed for initial conditions belonging to a small neighborhood of the attractor. On the other hand, the convergence time may be arbitrarily long for initial conditions located very close to one of the unstable periodic orbits. An important property of a periodic attractor is the average convergence time τ_{aver} defined as the average number of iterations of the return map needed to reach the attractor starting from random initial conditions. An estimate of the average convergence time can be computed as

$$\tau_{\text{aver}} \approx \frac{1}{K} \sum_{k=1}^K \tau(u_k), \quad (4)$$

where $\tau(u_k)$ are convergence times for trajectories started at randomly selected initial points u_1, u_2, \dots, u_K . The results obtained for selected periodic attractors existing for $R \in [2.099, 2.101]$ are presented in Table V. During the computations $K = 100$ initial points are tested. For each attractor we report the parameter value R , the period p , the average convergence time τ_{aver} , the maximum convergence time τ_{max} and the width w of the corresponding periodic window. Note that the average convergence time grows with

the period p and for periods $p \geq 13$ the average convergence time exceeds 10^5 . Finding periodic attractors with such a large convergence times using the standard approach would require computation of very long trajectories. Recall that in the brute force approach, trajectories of the length 20000 were computed. This explains the low number of periodic windows found using the standard approach.

TABLE V
CONVERGENCE TIMES FOR SELECTED CYCLES.

| R | p | τ_{aver} | τ_{max} | w |
|-----------------|-----|----------------------|---------------------|-------------------------|
| 2.100973 | 6 | 3.5×10^2 | 2.3×10^3 | 1.584×10^{-5} |
| 2.0996 | 7 | 9.4×10^2 | 4.5×10^3 | 2.711×10^{-6} |
| 2.1001625 | 8 | 2.2×10^3 | 1.1×10^4 | 4.478×10^{-7} |
| 2.0992159 | 9 | 3.7×10^3 | 1.6×10^4 | 1.276×10^{-7} |
| 2.1007698 | 10 | 2.9×10^3 | 1.6×10^4 | 2.756×10^{-7} |
| 2.09907145 | 11 | 1.4×10^4 | 7.3×10^4 | 1.182×10^{-8} |
| 2.099317506 | 12 | 3.8×10^4 | 1.7×10^5 | 2.060×10^{-9} |
| 2.0991612228 | 13 | 1.5×10^5 | 1.1×10^6 | 2.808×10^{-10} |
| 2.09935820935 | 14 | 2.6×10^5 | 2.0×10^6 | 6.848×10^{-11} |
| 2.100832505 | 15 | 2.6×10^5 | 1.2×10^6 | 4.077×10^{-10} |
| 2.1007717815 | 16 | 5.4×10^5 | 2.3×10^6 | 1.343×10^{-10} |
| 2.10077572841 | 17 | 1.2×10^6 | 5.8×10^6 | 2.043×10^{-11} |
| 2.0990506874954 | 18 | 4.5×10^6 | 2.0×10^7 | 3.770×10^{-13} |
| 2.100738098298 | 19 | 1.9×10^6 | 1.0×10^7 | 7.852×10^{-12} |
| 2.100828953277 | 20 | 5.3×10^6 | 2.5×10^7 | 2.949×10^{-13} |

Also note that the reduction of the window width w corresponds to the growth of the average convergence time τ_{aver} (compare Table V). This means that the two reasons which make it difficult to locate narrow periodic windows happen simultaneously. Narrow windows require dense sampling of the parameter space and long integration time to reach the corresponding periodic attractor.

V. CONCLUSIONS

A novel systematic approach based on the continuation method to locate periodic windows was introduced. The usefulness of the proposed approach was shown by locating a large number of periodic windows in bifurcation diagrams of the Chua's circuit. Measures of the set of regular parameters were estimated. Properties of periodic windows including their width were studied using the continuation method. Average convergence times for selected periodic attractors were computed numerically. The results obtained confirm that attractors in narrow periodic windows have large convergence times, which makes them difficult to detect using the standard method of monitoring trajectories. The proposed method is general; it can be used without modifications to study other dynamical systems.

REFERENCES

- [1] L. O. Chua, M. Komuro, and T. Matsumoto, "The double scroll family," *IEEE Trans. Circuits Syst.*, vol. 33, pp. 1037–1118, Nov. 1986.
- [2] M. Broucke, "One parameter bifurcation diagram for Chua's circuit," *IEEE Transactions on Circuits and Systems*, vol. 34, no. 2, pp. 208–209, 1987.
- [3] F. Bizzarri, D. Stellardo, and M. Storace, "Bifurcation analysis and its experimental validation for a hysteresis circuit oscillator," *IEEE Transactions on Circuits and Systems II: Express Briefs*, vol. 53, no. 7, pp. 517–521, 2006.
- [4] Y. Yamashita and H. Torikai, "A novel PWC spiking neuron model: Neuron-like bifurcation scenarios and responses," *IEEE Transactions on Circuits and Systems I: Regular Papers*, vol. 59, no. 11, pp. 2678–2691, 2012.
- [5] S. Kapat, "Sampling-induced border collision bifurcation in a voltage-mode dpwm synchronous buck converter," *IEEE Transactions on Circuits and Systems II: Express Briefs*, vol. 66, no. 6, pp. 1048–1052, 2019.
- [6] E. Lenz, D. J. Pagano, A. Ruseler, and M. L. Heldwein, "Two-parameter stability analysis of resistive droop control applied to parallel-connected voltage-source inverters," *IEEE Journal of Emerging and Selected Topics in Power Electronics*, vol. 8, no. 4, pp. 3318–3332, 2020.
- [7] W. Marszalek and J. Sadecki, "Complex two-parameter bifurcation diagrams of a simple oscillating circuit," *IEEE Transactions on Circuits and Systems II: Express Briefs*, vol. 66, no. 4, pp. 687–691, 2019.
- [8] A. Pala and M. Machaczek, "Computing of 3d bifurcation diagrams with nvidia cuda technology," *IEEE Access*, vol. 8, pp. 157 773–157 780, 2020.
- [9] M. Hénon, "A two dimensional map with a strange attractor," *Commun. Math. Phys.*, vol. 50, pp. 69–77, 1976.
- [10] R. May, "Simple mathematical models with very complicated dynamics," *Nature*, vol. 261, pp. 459–467, 1976.
- [11] A. El Aroudi, E. Rodríguez, R. Leyva, and E. Alarcon, "A design-oriented combined approach for bifurcation prediction in switched-mode power converters," *IEEE Transactions on Circuits and Systems II: Express Briefs*, vol. 57, no. 3, pp. 218–222, 2010.
- [12] B. Bao, N. Wang, Q. Xu, H. Wu, and Y. Hu, "A simple third-order memristive band pass filter chaotic circuit," *IEEE Transactions on Circuits and Systems II: Express Briefs*, vol. 64, no. 8, pp. 977–981, 2017.
- [13] P. Z. Wiecek and K. Gołofit, "True random number generator based on flip-flop resolve time instability boosted by random chaotic source," *IEEE Transactions on Circuits and Systems I: Regular Papers*, vol. 65, no. 4, pp. 1279–1292, 2018.

- [14] N. Nguyen, L. Pham-Nguyen, M. B. Nguyen, and G. Kaddoum, "A low power circuit design for chaos-key based data encryption," *IEEE Access*, vol. 8, pp. 104 432–104 444, 2020.
- [15] S. Chen, S. Yu, J. Lu, G. Chen, and J. He, "Design and FPGA-based realization of a chaotic secure video communication system," *IEEE Transactions on Circuits and Systems for Video Technology*, vol. 28, no. 9, pp. 2359–2371, 2018.
- [16] C. S. Kuka, Y. Hu, Q. Xu, and M. Alkahtani, "An innovative near-field communication security based on the chaos generated by memristive circuits adopted as symmetrical key," *IEEE Access*, vol. 8, pp. 167 975–167 984, 2020.
- [17] Z. Galias and W. Tucker, "Is the Hénon attractor chaotic?" *Chaos: Interdiscipl. J. Nonlinear Sci.*, vol. 25, no. 3, p. 033102 (12 pages), 2015.
- [18] T. Matsumoto, L. O. Chua, and M. Komuro, "The double scroll," *IEEE Trans. Circuits Syst.*, vol. 32, no. 8, pp. 798–817, Aug. 1985.
- [19] F. Ayrom and G. Zhong, "Chaos in Chua's circuit," *IEE Proceedings D - Control Theory and Applications*, vol. 133, no. 6, pp. 307–312, 1986.
- [20] M. Komuro, R. Tokunaga, T. Matsumoto, L. O. Chua, and A. Hotta, "Global bifurcation analysis of the double scroll circuit," *Int. J. Bifurcation Chaos*, vol. 1, no. 1, pp. 139–182, 1991.
- [21] S. Boughaba and R. Lozi, "Fitting trapping regions for Chua's attractor — a novel method based on isochronic lines," *Int. J. Bifurcation Chaos*, vol. 10, no. 1, pp. 205–225, 2000.
- [22] Y. Yang, Z. Duan, and L. Huang, "Robust dichotomy analysis and synthesis with application to an extended Chua's circuit," *IEEE Trans. Circuits Syst. I*, vol. 54, no. 9, pp. 2078–2086, 2007.
- [23] T. Matsumoto, L. O. Chua, and K. Ayaki, "Reality of chaos in the double scroll circuit: A computer-assisted proof," *IEEE Trans. Circuits Syst.*, vol. 35, no. 7, pp. 909–925, Jul. 1988.
- [24] Z. Galias, "Positive topological entropy of Chua's circuit: A computer assisted proof," *Int. J. Bifurcation Chaos*, vol. 7, no. 2, pp. 331–349, 1997.
- [25] Y. Liu, H. H. C. Iu, H. Li, and X. Zhang, "Bounded orbits and multiple scroll coexisting attractors in a dual system of chua system," *IEEE Access*, vol. 8, pp. 147 907–147 918, 2020.
- [26] A. Khibnik, D. Roose, and L. O. Chua, "On periodic and homoclinic bifurcations in Chua's circuits with a smooth nonlinearity," *Int. J. Bifurcation Chaos*, vol. 3, no. 2, pp. 363–384, 1993.
- [27] Z. Galias, "Rigorous analysis of Chua's circuit with a smooth nonlinearity," *IEEE Trans. Circuits Syst. I*, vol. 63, no. 12, pp. 2304–2312, Dec 2016.
- [28] Z. Galias and W. Tucker, "Rigorous integration of smooth vector fields around spiral saddles with an application to the cubic Chua's attractor," *Journal of Differential Equations*, vol. 266, no. 5, pp. 2408–2434, 2019.
- [29] G. Leonov, N. Kuznetsov, and V. Vagitsev, "Hidden attractor in smooth Chua systems," *Physica D: Nonlinear Phenomena*, vol. 241, no. 18, pp. 1482–1486, 2012.
- [30] Z. Galias, "Study of periodic windows for the Chua's circuit with a cubic nonlinearity," in *Proc. IEEE Int. Symp. Circuits Syst. (ISCAS)*, 2020, pp. 1–5.
- [31] —, "Systematic search for wide periodic windows and bounds for the set of regular parameters for the quadratic map," *Chaos: Interdiscipl. J. Nonlinear Sci.*, vol. 27, no. 5, p. 053106, 2017.



Zbigniew Galias (M'1992, SM'2013) received the M. Sc. degree in electronics from the AGH University of Science and Technology, Kraków, Poland in 1990, the M. Sc. degree in mathematics from the Jagiellonian University, Kraków, Poland in 1992, the Ph. D. degree and the senior doctorate degree in electrical engineering from the AGH University of Science and Technology, Kraków, Poland in 1996 and 2004. In 2015, he received the title of Professor.

He is currently a full professor at the Department of Electrical Engineering and Power Engineering, AGH University of Science and Technology, Kraków, Poland. His research interests include complex and nonlinear circuits and systems, chaos, computer assisted proofs, power networks and sliding mode control.

Prof. Galias served/is serving as an Associate Editor of the *IEEE Transactions on Circuits and Systems I and II*, *IEEE Circuits and Systems Magazine*, and the *International Journal of Bifurcation and Chaos*.